Biodistribution and Imaging Studies of Technetium-99m-Labeled Liposomes in Rats with Focal Infection

Beth Goins, Robert Klipper, Alan S. Rudolph, Richard O. Cliff, Ralph Blumhardt and William T. Phillips

Radiology Department, University of Texas Health Science Center at San Antonio, San Antonio, Texas and Center for Biomolecular Science and Engineering, Naval Research Laboratory, Washington, D.C.

We have recently developed a procedure to label liposomes containing reduced glutathione (GSH) with ^{99m}Tc using the lipophilic chelator, hexamethylpropyleneamine oxime (HMPAO). In the present study, we evaluated the use of ^{99m}Tc-liposomes to detect focal infection sites in rats. Rats were infected in the thigh by intramuscular injection with *Staphylococcus aureus* followed 24 hr later by an intravenous injection of ^{99m}Tc-liposomes, ^{67}Ga-citrate, or ^{99m}Tc-human serum albumin (HSA). The animals were imaged under a gamma camera and subsequently killed at 4, 24 or 48 hr for tissue biodistribution studies. In contrast to infected rats receiving ^{67}Ga-citrate or ^{99m}Tc-HSA, abscesses were prominently localized within 2 hr in rats after ^{99m}Tc-liposome injection, and continued to increase in activity up to 24 hr. Abscess-to-muscle ratios calculated from 24-hr biodistribution data obtained from tissue sampling were 35.3 ± 7.6 for ^{99m}Tc-liposomes, 4.1 ± 0.7 for ^{67}Ga-citrate and 8.0 ± 1.0 for ^{99m}Tc-HSA. These studies show the potential of using ^{99m}Tc-liposomes to localize infection.

J Nucl Med 1993; 34:2160–2168

The utility of radiopharmaceutical agents for the noninvasive detection of infection sites has received considerable attention, particularly in the septic postoperative patient, because of the need to quickly and accurately identify the infected area for drainage (*1*). Gallium-67-citrate and ^{111}In-labeled leukocytes remain the most common agents in the clinical setting despite a number of associated problems, including poor imaging and dosimetry characteristics, nonspecific localization to other pathological areas such as tumors and inflammation, laborious leukocyte separation procedures and potential exposure to contaminated blood products (*2–5*). Both of these agents also require a 24-hr lag period between administration and imaging to reduce background activity, which may be too long in some situations. Technetium-99m-albumin nanocolloid and ^{99m}Tc-human serum albumin (HSA) have been evaluated as substitutes for ^{111}In-labeled leukocytes because they are readily available and convenient to label (*6,7*). Other radiopharmaceuticals for infection imaging are under development, including polyclonal IgG labeled with ^{111}In (*8–11*) and ^{99m}Tc (*12,13*) as well as leukocytes labeled with ^{99m}Tc (*14*).

Liposomes, spherical lipid bilayers which can carry a variety of drugs or radionuclides within their aqueous space, are another agent with potential diagnostic imaging applications (*15–17*). In this paper, we have used ^{99m}Tc-liposomes labeled with a method (*18,19*) to detect focal infection sites in rats. This procedure uses the lipophilic chelator, hexamethylpropyleneamine oxime (HMPAO) to carry ^{99m}Tc inside preformed liposomes containing reduced glutathione (GSH). The ^{99m}Tc-HMPAO molecule is thought to be chemically reduced in the presence of the GSH, becoming more hydrophilic and therefore trapped within the liposome. This proposed liposome labeling mechanism may be similar to the mechanism of intracellular trapping of ^{99m}Tc-HMPAO by high concentrations of GSH in the brain (*20,21*). The advantages of this system are that the ^{99m}Tc-liposomes are easy to label, have a high labeling efficiency and would be readily available in kit form. Another advantage of this ^{99m}Tc liposome labeling technique appears to be that the ^{99m}Tc label is retained at the site of liposome deposition for prolonged periods without rapid metabolism. The prolonged retention results in improved image quality. In the present study, ^{99m}Tc-liposomes were directly compared to ^{67}Ga-citrate and ^{99m}Tc-HSA in a rat infection model. The results from this study indicate that ^{99m}Tc-liposomes labeled with this procedure are superior to the common radiopharmaceuticals used for infection imaging and could replace labeled leukocytes in the localization of focal infection sites in certain situations.

MATERIALS AND METHODS

Liposome Preparation

The liposomes were produced and characterized as previously outlined (*18,19*). The phospholipids distearoyl phosphatidylcholine (DSPC) and dimyristoyl phosphatidylglycerol (DMPG) were purchased from Avanti Polar Lipids (Pelham, AL). Cholesterol was obtained from Calbiochem (La Jolla, CA) and α-tocopherol

Received Feb. 18, 1993; revision accepted Aug. 5, 1993.

For correspondence and reprint contact: William T. Phillips, MD, Radiology Department, University of Texas Health Science Center at San Antonio, 7703 Floyd Curl Dr., San Antonio, TX 78284-7800.

was purchased from Aldrich (Waukegan, IL). All liposomes used in this study were prepared by co-drying the lipids from chloroform prior to rehydration with 30 m*M* reduced glutathione (Sigma, St. Louis, MO) in Dulbecco's phosphate-buffered saline (PBS), pH 7.4. The resultant multilamellar liposomes were passed through a microfluidizer (Microfluidics, Newton, MA) to form smaller and more unilamellar liposomes. After processing, the liposomes were diluted with PBS, pH 7.4, and spun at 70,000 rpm in a Beckman ultracentrifuge for 1 hr to remove any extravesicular GSH. For this study, all liposomes were comprised of DSPC: cholesterol: DMPG: α-tocopherol (50:38:10:2 molar ratio). Liposomal size was monitored using a Coulter N4-MD particle size analyzer (Hileah, FL). Phospholipid content of the liposomes was assayed using the method by Stewart (*22*). Liposomes were assayed for endotoxin and bacterial contamination on fluid thioglycollate media prior to labeling and injection. The intravesicular concentration of GSH has been estimated at 1.2 m*M* using [^{3}H]GSH (Du Pont New England Nuclear, Boston, MA) (*18*).

Labeling Procedures

The ^{99m}Tc labeling procedure for preformed liposomes recently has been described (*18*). Briefly, approximately 10 ml of liposomes containing GSH were mixed with an HMPAO kit (Ceretec, Amersham, Arlington Heights, IL) preincubated with 10 mCi of sodium pertechnetate in 5 ml of 0.9% saline. The reconstituted kits were checked for contamination by free pertechnetate, reduced hydrolyzed ^{99m}Tc and hydrophilic ^{99m}Tc-HMPAO complex with the active lipophilic ^{99m}Tc-HMPAO complex using a three-step thin-layer chromatography system outlined in the HMPAO kit package insert. In all cases, the kits used for the liposome labeling studies contained >80% lipophilic HMPAO, as recommended for clinical brain studies. After a 30-min incubation, the liposomes were separated from any free ^{99m}Tc by passage over a Sephadex G-25 column. Labeling efficiencies were checked by determining the activity before and after column separation of the ^{99m}Tc-liposomes using a dose calibrator (Radex Model Mark 5, Houston, TX). Also, chromatography on Schleicher and Schuell #589 white ribbon paper developed in 0.9% saline was performed on pre- and post-column samples (*23*). With this technique, the liposomes remain at the origin, while both free ^{99m}Tc and ^{99m}Tc-HMPAO move with the solvent front. The labeling efficiency of the post-column fractions of ^{99m}Tc-liposomes was >85%. The post-column preparations of ^{99m}Tc-liposomes were used immediately for injection.

Gallium-67-citrate (Du Pont, Billerica, MA) and ^{99m}Tc-HSA (Medi Physics, Arlington Heights, IL) were purchased in kit form and reconstituted by Syncor (San Antonio, TX). An aliquot was taken and diluted with 0.9% saline prior to injection.

Infection Model

The animal experiments were performed under the National Institutes of Health Animal Use and Care guidelines and were approved by the University of Texas Health Science Center at San Antonio Institutional Animal Care Committee. *Staphylococcus aureus* (ATCC strain 19095) was rehydrated from a lyophilized powder and grown in trypticase soy broth overnight in a 37°C shaking water bath prior to harvesting by centrifugation. The number of bacterial cells was estimated by counting an aliquot of the diluted cell suspension in a hemocytometer. Male Sprague-Dawley rats (250–300 g) were injected intramuscularly in the thigh with 5.6×10^8 bacterial cells in 0.2 ml complete Freund's adjuvant. Twenty-four hours later, swelling in the infected thigh was noted. The infected rats were anesthetized with Metofane (Pitman-Moore, Mundelein, IL) and injected intravenously in the tail vein with an average dose of 300 μCi ^{67}Ga-citrate, 400 μCi ^{99m}Tc-HSA or 233 μCi ^{99m}Tc-liposomes in a volume of 2 ml. Two rats served as controls and received only 0.2 ml of complete Freund's adjuvant 24 hr prior to ^{99m}Tc-liposome injection. The ^{99m}Tc-liposomes used in this study had an average size of 185 nm by unimodal analysis of laser light scattering data. The phospholipid dose was 125 mg phospholipid/kg body weight.

Imaging Acquisition and Analysis

At 0.5, 1, 2, 4, 24 and 48 hr, the rats were anesthetized with Metofane and placed in the prone position for the imaging studies. Whole-body scintigrams were acquired using a Searle Radiographics Model 6413 gamma camera equipped with a low-energy, all-purpose collimator for the ^{99m}Tc studies or a medium-energy collimator for the ^{67}Ga-citrate studies. The camera was interfaced to a Pinnacle computer (Medasys, Ann Arbor, MI) and 1-min static images were acquired using a 64 × 64 matrix. Five-minute static images were acquired at 24 hr for rats injected with ^{99m}Tc-liposomes and ^{99m}Tc-HSA due to loss of signal from isotope decay. The animals were housed immediately in metabolic cages after receiving the radiopharmaceutical and remained there until tissue biodistribution at 4, 24 or 48 hr.

Regions of interest were drawn around the infected area of the thigh (target) and a comparable zone in the contralateral thigh (background) observed in the rat images using the Pinnacle software. A box was drawn around the entire body to determine total body counts. The target-to-background ratio was calculated using the following equation:

$$\text{Target-to-Background Ratio} = \frac{\text{Counts (infected thigh)}}{\text{Counts (uninfected thigh)}}.$$

Also the activity in the infected thigh at various times was determined using the equation:

$$\%\ \text{activity in infected thigh} = \frac{\text{Counts (infected thigh)}}{\text{Counts (total body)}} \times 100.$$

Biodistribution Studies

After imaging, the animals were anesthetized with Metofane and a blood sample was obtained by cardiac puncture prior to death by cervical dislocation. Tissue samples were excised, thoroughly washed with saline and weighed. Samples of each organ were counted in a scintillation well counter (Canberra Multichannel Analyzer, Meridian, CT). A small sample of each radiopharmaceutical (50 μl for ^{67}Ga-citrate, 500 μl for ^{99m}Tc-HSA and 300 μl ^{99m}Tc-liposomes) was placed in a plastic cuvette and used as a standard reference. Organ and fluid counts too high for detection at the time of death were stored until decay allowed for accurate determination. Bowel activity was determined by counting an aliquot of bowel digest after the total bowel plus contents and was heated in the presence of saturated NaOH. Total blood volume, bone, muscle, brain and skin mass were estimated as 5.4%, 10%, 40%, 0.7% and 13% of total body weight, respectively (*24,25*).

Histopathological Studies

Samples of infected and contralateral normal thigh muscle were taken for histopathological examination. The samples were frozen and sectioned prior to staining with hemoxylin/eosin or with Oil Red O for lipid staining. The prepared slides were viewed using a Nikon Optiphot light microscope with a camera attachment.

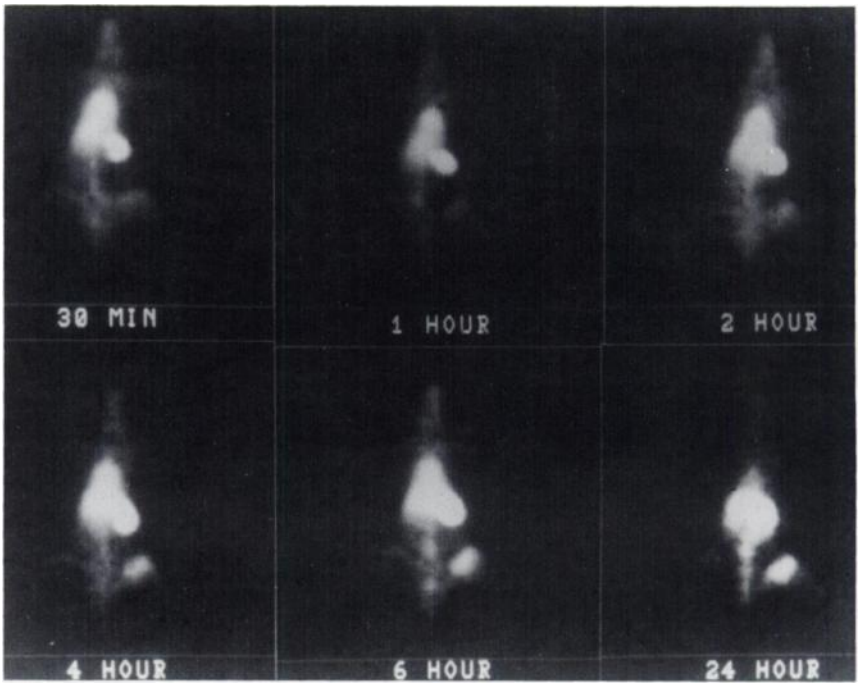

FIGURE 1. Serial whole-body gamma camera images showing the increased accumulation of ^{99m}Tc-liposomes in a rat with a *Staphylococcus aureus* thigh abscess over a 24-hr period.

Statistical Methods

Values are reported as mean ± standard error of the mean. Target-to-background ratios, percent activity in the abscess and abscess-to-muscle ratios were compared for each radiopharmaceutical and at different time points using the Student's unpaired t-test. The acceptable probability for a significant difference between means was $p < 0.05$.

RESULTS

Figure 1 shows the time course of accumulation over a 24-hr period of ^{99m}Tc-liposomes in the rat thigh previously infected with *Staphylococcus aureus*. By 2 hr, the abscess can be delineated from the background muscle activity and becomes more prominent with time. The other major areas of accumulation are the reticuloendothelial system organs of the liver and spleen, which are normal sites of clearance for liposomes (*26*). Also note the large amount of activity localized in the heart, representative of the cardiac blood pool. No significant activity was seen in the bladder, kidneys, thyroid or stomach, thus showing the excellent in vivo stability of ^{99m}Tc-liposomes using the labeling procedure outlined in this paper.

Target-to-background ratios were calculated from the images acquired over the 24-hr period. As depicted in Figure 2A, the ^{99m}Tc-liposomes have a target-to-background ratio of 2.9 ± 0.3 at 2 hr, which continues to increase to a significantly greater value of 6.9 ± 1.1 by 24 hr postinjection ($p < 0.05$). Rats ($n = 2$) injected with adjuvant alone and infused with an equivalent dose of ^{99m}Tc-liposomes were also imaged under the gamma camera. The target-to-background ratio was 2.0 ± 0.2 at 2 hr and 5.2 ± 1.9 at 24 hr for the adjuvant alone rats.

The percent of the activity in the abscess compared to the total body counts (Fig. 2B) also increased over the 24-hr period. There was 4.6% ± 0.4% of the total body

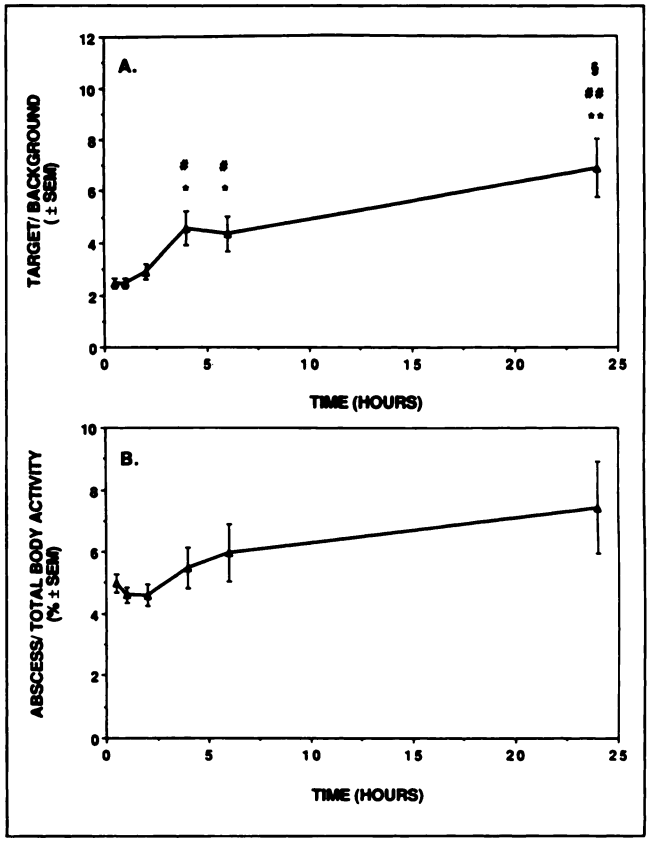

FIGURE 2. (A) Target-to-background ratios calculated from ROI image analysis of rats ($n = 4$) with a focal infection injected with ^{99m}Tc-liposomes and imaged over a 24-hr period. (B) Activity in the abscess of infected rats ($n = 4$) injected with ^{99m}Tc-liposomes compared to total body activity over a 24-hr period. The activity was determined from ROI image analysis. The values represent the mean ± s.e.m. Differences considered to be statistically significant are indicated as follows: *, $p < 0.05$ versus 0.5 hr; #, $p < 0.05$ versus 1 hr; §, $p < 0.05$ versus 2 hr; **, $p < 0.01$ versus 0.5 hr; ##, $p < 0.01$ versus 1 hr.

TABLE 1
Tissue Biodistribution of ^{99m}Tc-Liposomes

Organ	4 hr (n = 4)		24 hr (n = 9)		48 hr (n = 4)	
	%/Organ	%/Gram tissue	%/Organ	%/Gram tissue	%/Organ	%/Gram tissue
Spleen	23.1 ± 1.4	29.2 ± 0.9	26.8 ± 1.8	38.9 ± 5.7	16.2 ± 0.5	24.3 ± 1.0
Lung	0.8 ± 0.1	0.6 ± 0.1	0.5 ± 0.04	0.3 ± 0.03	0.3 ± 0.03	0.2 ± 0.02
Liver	11.9 ± 0.4	1.1 ± 0.01	10.4 ± 0.3	1.0 ± 0.1	6.3 ± 0.4	0.5 ± 0.03
Blood	30.9 ± 0.1	2.0 ± 0.1	13.4 ± 1.7	0.8 ± 0.1	3.8 ± 0.4	0.3 ± 0.02
Testis	0.1 ± 0.01	0.04 ± 0.003	0.1 ± 0.01	0.02 ± 0.002	0.1 ± 0.004	0.02 ± 0.01
Femur	6.2 ± 0.5	0.2 ± 0.02	6.1 ± 0.5	0.2 ± 0.01	3.7 ± 0.3	0.1 ± 0.01
Heart	0.2 ± 0.01	0.2 ± 0.01	0.1 ± 0.01	0.1 ± 0.01	0.1 ± 0.004	0.1 ± 0.003
Brain	0.1 ± 0.01	0.1 ± 0.01	0.05 ± 0.004	0.03 ± 0.002	0.03 ± 0.01	0.02 ± 0.003
Skin	2.3 ± 0.2	0.1 ± 0.01	2.6 ± 0.5	0.1 ± 0.01	2.5 ± 0.4	0.1 ± 0.01
Kidney	2.5 ± 0.3	1.2 ± 0.1	3.5 ± 0.2	1.7 ± 0.1	4.3 ± 0.1	2.1 ± 0.1
Urine	6.3 ± 0.6	0.2 ± 0.04	14.3 ± 1.1	0.5 ± 0.1	26.6 ± 1.5	0.6 ± 0.1
Bowel	5.4 ± 0.2	0.2 ± 0.01	4.1 ± 0.3	0.1 ± 0.02	3.3 ± 0.2	0.1 ± 0.003
Feces	*	*	2.8 ± 1.1	0.6 ± 0.2	8.7 ± 1.0	1.2 ± 0.2
Muscle	2.2 ± 0.2	0.02 ± 0.002	2.0 ± 0.2	0.02 ± 0.001	0.1 ± 0.1	0.01 ± 0.001
Abscess	1.4 ± 0.1	0.2 ± 0.04	2.3 ± 0.4	0.5 ± 0.1	2.6 ± 0.5	0.4 ± 0.1
Abscess-to-Muscle ratio	—	10.5 ± 2.6	—	35.3 ± 7.6	—	38.9 ± 9.4

*Not measured.
Values represent the mean ± standard error.

counts in the abscess at 2 hr, which increased to 7.4% ± 1.5% by 24 hr. The activity compared to the total body counts for the rats receiving adjuvant alone at 2 hr was 3.9% ± 0.3% and increased to 4.9% ± 1.9% by 24 hr. There were no significant effects of time in the percent activity in the infected area compared to the total body counts for the rats receiving *Staphylococcus aureus*.

As outlined in Table 1, tissue biodistribution data for ^{99m}Tc-liposomes for rats killed at 4, 24 and 48 hr postinjection also showed increasing abscess-to-muscle ratios over time due to increased activity in the abscess with a decrease in muscle activity with time. The abscess-to-muscle ratios for ^{99m}Tc-liposomes of 35.3 ± 7.6 at 24 hr ($p < 0.05$) and 38.9 ± 9.4 at 48 hr ($p < 0.025$) were significantly greater than the ratio of 10.5 ± 2.6 at 4 hr. Although the abscess-to-muscle ratio continued to increase from 24 hr to 48 hr, this difference was not statistically significant. Activities determined from excised tissue also confirm the image organ distribution pattern with predominant activity in the blood pool and reticuloendothelial organs.

The ^{99m}Tc-liposomes were also compared to two other radiopharmaceuticals used in infection imaging, ^{67}Ga-citrate and ^{99m}Tc-HSA, as shown in the gamma camera images depicted in Figure 3. At 4 hr postinjection, both ^{99m}Tc-liposomes (Fig. 3C) and ^{99m}Tc-HSA (Fig. 3B) showed prominent accumulation at the infected site. Yet, by 24 hr,

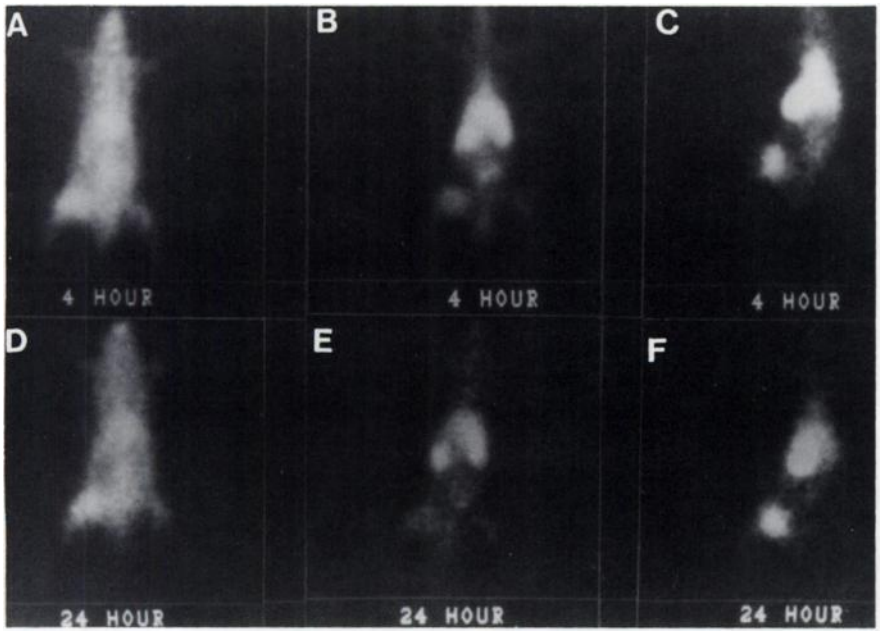

FIGURE 3. Gamma camera images of rats with a *Staphylococcus aureus* thigh abscess imaged following intravenous injection of ^{67}Ga-citrate (A, 4 hr; D, 24 hr), ^{99m}Tc-HSA (B, 4 hr; E, 24 hr) or ^{99m}Tc-liposomes (C, 4 hr; F, 24 hr).

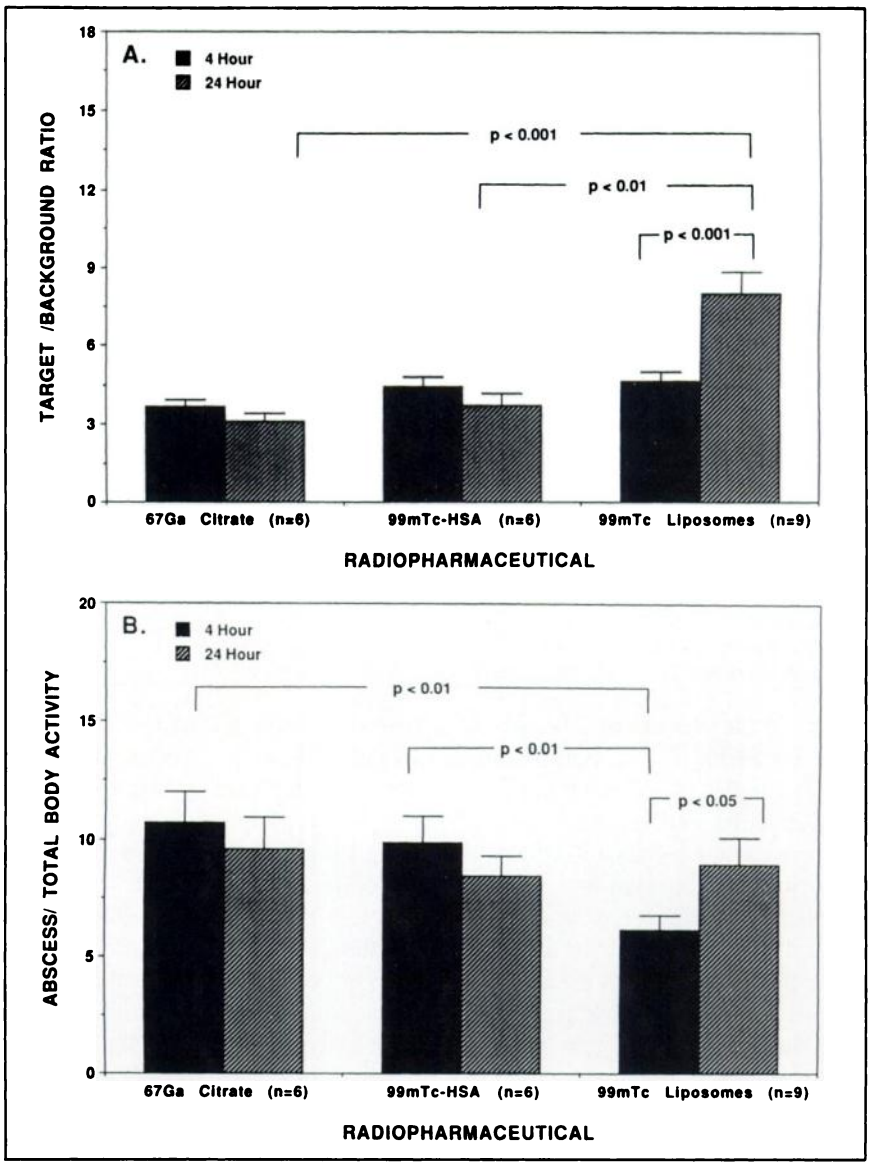

FIGURE 4. Comparison of target-to-background ratios (A) and percent activity in abscess (B) determined from ROI analysis of scintigrams of infected rats following injection of ^{67}Ga-citrate (n = 6), ^{99m}Tc-HSA (n = 6) or ^{99m}Tc-liposomes (n = 9). The values represent the mean ± s.e.m. Differences considered to be statistically significant are indicated.

^{99m}Tc-HSA (Fig. 3E) had decreased activity at the abscess, while the ^{99m}Tc-liposomes (Fig. 3F) continued to accumulate at the infected site. In contrast to the images of the ^{99m}Tc radiopharmaceuticals, which have ideal imaging energy characteristics, the ^{67}Ga-citrate images (Figs. 3A and D) were not as clear and changed very little over the 24-hr period due to the much longer half-life (68 hr) of ^{67}Ga. Although the abscess located in the thigh was noticeable at 4 and 24 hr in rats injected with ^{67}Ga-citrate, the large background contribution of muscle and bowel greatly reduced the detectability of the infection site.

Target-to-background ratios calculated from ROI image analysis for the radiopharmaceutical comparison study are depicted in Figure 4A. Although similar ratios ranging from 3.7 ± 0.3 to 4.6 ± 0.4 for the three radiopharmaceuticals were determined at 4 hr postinjection, by 24 hr, the ^{99m}Tc-liposomes continued to accumulate at the infected site. The target-to-background ratio for ^{99m}Tc-liposomes doubled from 4.6 ± 0.4 at 4 hr to a significant value of 8.0 ± 0.8 at 24 hr ($p < 0.001$). In contrast to the increased target-to-background ratio for ^{99m}Tc-liposomes, the target-to-background ratios of ^{99m}Tc-HSA and ^{67}Ga-citrate decreased slightly to 3.7 ± 0.4 and 3.1 ± 0.3 at 24 hr, respectively. There was no significant effect of time on the target-to-background ratio for both ^{99m}Tc-HSA or ^{67}Ga-citrate.

Figure 4B shows the percent of activity in the abscess compared to total body activity for the three radiopharmaceuticals. At 4 hr postinjection, both the ^{67}Ga-citrate and ^{99m}Tc-HSA percentages of 9.9% ± 1.1% and 10.7% ± 1.2%, respectively, were significantly greater ($p < 0.01$) than the ^{99m}Tc-liposome percentage of 6.1% ± 0.6%. Both the ^{67}Ga-citrate and ^{99m}Tc-HSA percentages decreased from 4 to 24 hr, and the differences were not statistically significant. However, the percentage of activity in the abscess to total body counts for ^{99m}Tc-liposomes increased over the same period from 6.1% ± 0.6% at 4 hr to a significantly different value of 9.0% ± 1.1% at 24 hr ($p < 0.05$).

TABLE 2
Tissue Biodistribution of Radiopharmaceuticals at 24 Hours Postinjection

Organ	^{67}Ga-citrate (n = 6)		^{99m}Tc-HSA (n = 6)		^{99m}Tc-Liposomes (n = 9)	
	%/Organ	%/Gram tissue	%/Organ	%/Gram tissue	%/Organ	%/Gram tissue
Spleen	1.8 ± 0.2	2.4 ± 0.3	1.8 ± 0.2	2.8 ± 0.5	26.8 ± 1.8	38.9 ± 5.7
Lung	0.4 ± 0.1	0.3 ± 0.04	0.2 ± 0.02	0.2 ± 0.01	0.5 ± 0.04	0.3 ± 0.03
Liver	12.7 ± 0.7	1.1 ± 0.06	8.7 ± 0.7	0.8 ± 0.1	10.4 ± 0.3	1.0 ± 0.1
Blood	1.9 ± 0.2	0.1 ± 0.01	2.7 ± 0.4	0.2 ± 0.02	13.4 ± 1.7	0.8 ± 0.1
Testis	0.9 ± 0.1	0.2 ± 0.03	0.5 ± 0.02	0.1 ± 0.01	0.1 ± 0.01	0.02 ± 0.002
Femur	37.5 ± 3.4	1.3 ± 0.1	8.4 ± 0.8	0.3 ± 0.03	6.1 ± 0.5	0.2 ± 0.01
Heart	0.3 ± 0.04	0.3 ± 0.04	0.2 ± 0.004	0.1 ± 0.004	0.1 ± 0.01	0.1 ± 0.01
Brain	0.9 ± 0.01	0.04 ± 0.01	0.02 ± 0.001	0.01 ± 0.001	0.05 ± 0.004	0.03 ± 0.002
Skin	5.6 ± 0.7	0.3 ± 0.2	5.3 ± 1.5	0.1 ± 0.04	2.6 ± 0.5	0.1 ± 0.01
Kidney	1.5 ± 0.1	0.8 ± 0.1	7.3 ± 0.2	3.6 ± 0.1	3.5 ± 0.2	1.7 ± 0.1
Urine	7.1 ± 0.8	0.3 ± 0.02	27.6 ± 2.0	1.0 ± 0.1	14.3 ± 1.1	0.5 ± 0.1
Bowel	9.3 ± 0.5	0.3 ± 0.02	6.2 ± 0.8	0.1 ± 0.01	4.1 ± 0.3	0.1 ± 0.02
Feces	6.2 ± 1.8	2.8 ± 0.8	6.6 ± 1.0	2.7 ± 0.4	2.8 ± 1.1	0.6 ± 0.2
Muscle	17.1 ± 2.9	0.2 ± 0.03	3.0 ± 0.1	0.03 ± 0.001	2.0 ± 0.2	0.02 ± 0.001
Abscess	2.6 ± 0.5	0.6 ± 0.02	0.8 ± 0.1	0.2 ± 0.03	2.3 ± 0.4	0.5 ± 0.1
Abscess-to-Muscle Ratio	—	4.1 ± 0.7	—	8.0 ± 1.0	—	35.3 ± 7.6

Values represent the mean ± standard error.

Table 2 shows the tissue biodistribution data for the three experimental groups at 24 hr postinjection. Gallium-67-citrate accumulated predominately in the liver, femur, muscle and bowel. In contrast, the ^{99m}Tc radiopharmaceuticals had little muscle activity. The ^{99m}Tc-liposomes accumulated more in the reticuloendothelial organs of the spleen and liver than the water soluble ^{99m}Tc-HSA. Also, the ^{99m}Tc-radiopharmaceuticals excreted more activity in urine than ^{67}Ga-citrate.

The abscess-to-muscle ratios at 24 hr calculated from tissue biodistribution data for the three radiopharmaceuticals are shown in Figure 5. The abscess-to-muscle ratio for ^{99m}Tc-liposomes of 35.3 ± 7.6 was significantly greater than the ratio of 8.0 ± 1.0 for ^{99m}Tc-HSA ($p < 0.01$) and 4.1 ± 0.7 for ^{67}Ga-citrate ($p < 0.01$). Also, the ^{99m}Tc-HSA ratio was significantly greater than the ratio of ^{67}Ga-citrate at 24 hr ($p < 0.01$).

Histological sections stained with hemoxylin and eosin of the infected muscle from rats receiving a ^{99m}Tc-liposome injection 24 hr prior to death showed an infiltration of leukocytes in the infected muscle (Fig. 6A). Staining the same sections with Oil Red O showed lipid staining in the area of leukocyte infiltration which may represent liposomes (Fig. 6B). A further magnification of the area of leukocyte infiltration showed lipid stained areas around the leukocyte (Fig. 6C). It could not be determined from these photomicrographs if the red stained areas represented surface association or engulfment of the liposomes by the leukocytes.

DISCUSSION

Development of radiopharmaceuticals for the noninvasive detection of infection remains an active area of research (*27*). Although no one agent may serve all purposes, the ^{99m}Tc-liposomes evaluated in this report may be a useful addition to the list of radiopharmaceuticals available to clinicians for infection imaging. There are a number of advantages of ^{99m}Tc-liposomes for infection imaging. One important advantage is that the agent is labeled with ^{99m}Tc, which has an ideal dosimetry and imaging characteristics. The short half-life of ^{99m}Tc allows for imaging focal infections prior to 24 hr following administration for emergency situations. Also, preformed liposomes used in this ^{99m}Tc labeling protocol would be readily available either in solution or as a lyophilized powder, unlike leukocytes which

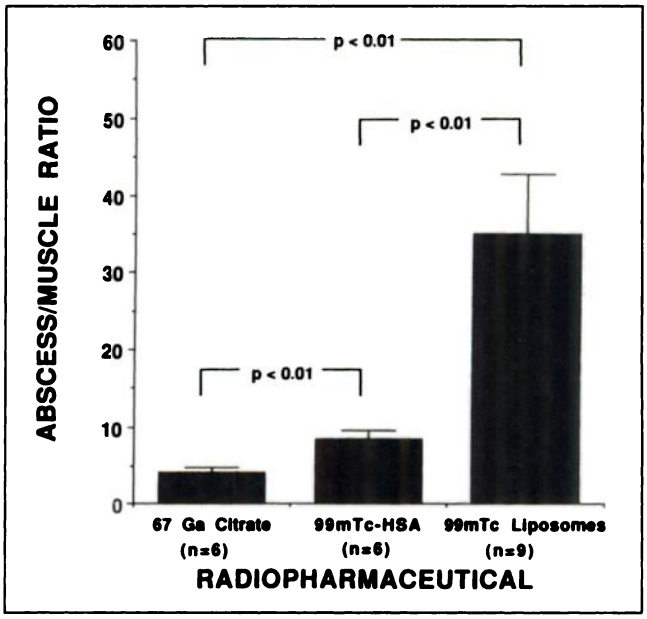

FIGURE 5. Abscess-to-muscle ratios calculated from tissue biodistribution data at 24 hr postinjection for ^{67}Ga-citrate (n = 6), ^{99m}Tc-HSA (n = 6) or ^{99m}Tc-liposomes (n = 9). The values represent the mean ± s.e.m. Differences considered to be statistically significant are indicated.

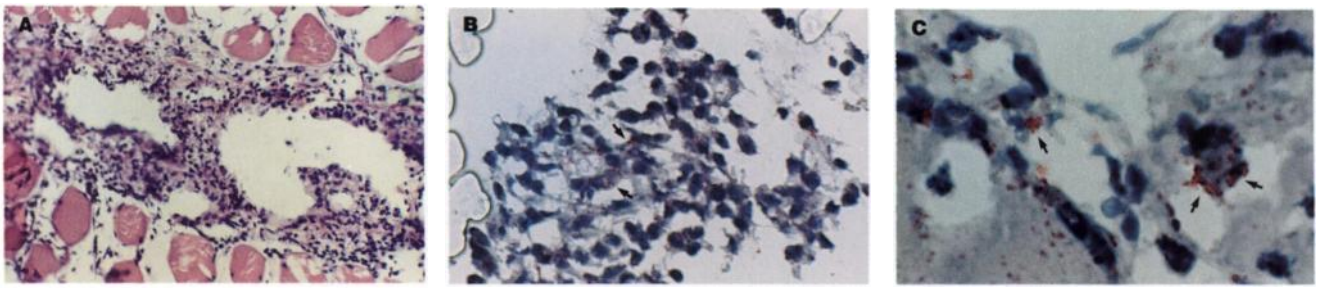

FIGURE 6. Photomicrographs taken of sectioned infected muscle from a rat that was injected with ^{99m}Tc-liposomes and killed 24 hr later. (A) Hemoxylin/eosin stained section showing the leukocyte infiltration surrounding the myocytes. Magnification 376×. (B) Oil Red O stained section showing the lipid staining red spherical areas in the leukocyte infiltration (see arrows). Magnification 781×. (C) Same section as in (B) but at higher magnification showing the lipid staining surrounding the leukocyte (see arrows). Magnification 1462×.

must be separated from other blood components prior to labeling. Liposomes have been shown to be stable when lyophilized in the presence of certain disaccharides, namely trehalose and sucrose (*28*). The use of lyophilization as a storage form for liposomes has been an important issue in the commercialization of liposomes as drug carriers (*29,30*). Additionally, the ^{99m}Tc-liposomes used in this study were easy to prepare and had a high labeling efficiency.

Liposomes labeled with ^{99m}Tc have previously been studied as a radiopharmaceutical for diagnostic infection imaging in both animal (*31*) and human models (*32*). These previous studies used large multilamellar liposomes which were predominately cleared from the blood pool into the reticuloendothelial cells of the liver and spleen. In contrast, the liposomes used in this study have been processed to a much smaller size to evade the reticuloendothelial system for a longer period of time. This allows labeled liposomes to remain in the blood pool, thus increasing the possibility of a liposome interaction with the infection site. In addition, the large multilamellar liposomes used in these early studies (*31,32*) were labeled with ^{99m}Tc by adding sodium pertechnetate to a preformed liposome suspension. This surface labeling procedure has been shown to be unstable with excessive loss of the label from the liposome (*33*). This instability was clearly seen in the images of infected rats with free ^{99m}Tc activity in the kidneys and bladder (*31*). In contrast, the labeling procedure used in this study is stable in vivo with little urinary excretion of ^{99m}Tc over a 24-hr period. These ^{99m}Tc-liposomes would be ideally suited for abdominal abscess localization because of the lack of bladder and kidney activity.

Concerns of any potential toxicities associated with the use of liposomes as drug or radiotracer carriers has received considerable attention as more liposomal-based products come to the marketplace (*34*). The effects on the host-defense function of the reticuloendothelial system due to a blockade or saturation by liposomes could play an important role in already compromised patients. Although these concerns have been warranted in the past, better manufacturing and quality control methods continue to be developed, with several liposome products currently in clinical trials for treatment of systemic fungal infections and cancer (*35,36*). In addition, second generation liposome formulations containing lipids with their headgroup region composed of sialic acid residues or polyethylene glycol moieties are being developed to better evade the reticuloendothelial system (*37,38*). Studies using these second generation liposomes could be attempted using the infection model outlined in this study. For the liposome formulation used in this study, histopathological and RES function studies have been conducted in rats (*39,40*). Accumulation of lipid in the liver and spleen was noted in stained tissue sections following a 25% blood volume infusion of the liposomes at the early time points, with recovery of normal histopathology occurring between 24 hr and 1 wk postinfusion (*39*). Animals challenged with carbon particles at various times following a 25% blood volume infusion of liposomes showed that there was a minimal decrease in the carbon clearance rate at 2 hr, which returned to normal values by 24 hr postinfusion (*40*).

The ^{99m}Tc-liposomes were compared with ^{99m}Tc-HSA, another agent used for infection imaging. Both agents have the advantage of being ^{99m}Tc-based. As noted in other comparison studies (*6,10*), ^{99m}Tc-HSA penetrated the capillary bed area due to increased vascular permeability and most likely was removed from the area by lymphatic drainage by 24 hr. On the contrary, the ^{99m}Tc-liposomes used in this study continued to accumulate up to 24 hr. The exact mechanism for the increased accumulation at the infection site is not known, but one possible explanation may be that the leukocytes in the area phagocytize the liposomes, trapping them within the area. Histopathological examination of infected muscle sections stained for lipid using Oil Red O indicated lipid staining in the area of leukocyte infiltration, which may represent liposomes. This staining technique was not sensitive enough to detect whether the liposomes were merely associated with the leukocyte surface or engulfed by the leukocytes.

The ability to perform imaging with ^{99m}Tc-liposomes as early as 4 hr and then rescan at 24 hr is an advantage when compared to infection imaging with ^{99m}Tc-HSA. HSA images revealed a significant amount of kidney activity not seen with ^{99m}Tc-liposomes. Like ^{99m}Tc-HSA, ^{99m}Tc-liposomes are nonspecific for inflammatory processes and

would probably not distinguish inflammations due to microorganisms from other causes of inflammation.

Direct comparison of ^{99m}Tc-liposomes with ^{67}Ga-citrate showed the liposome product to be superior in delineating the abscess at both 4 and 24 hr postinjection. The improved imaging and dosimetry characteristics of the ^{99m}Tc-liposomes over ^{67}Ga-citrate may play a major role in the increased ability to detect the infection site of rats administered the ^{99m}Tc-liposomes. The high bowel activity seen with ^{67}Ga-citrate compared to ^{99m}Tc-liposomes would make detection of intra-abdominal abscesses difficult. High background contribution of ^{67}Ga-citrate in the muscle when compared to both ^{99m}Tc-liposomes and ^{99m}Tc-HSA is a disadvantage and contributes to the decreased delineation of the abscess. One of the most striking aspects of this study was the high abscess-to-muscle ratio obtained with the ^{99m}Tc-liposomes at 24 hr as compared to ^{67}Ga-citrate or ^{99m}Tc-HSA. This ratio of 35.3 ± 7.6 is higher than all other infection detection agents except leukocytes reported in a recent study comparing various radiopharmaceuticals used for infection imaging in a dog model (*41*).

Human polyclonal antibody (IgG) labeled with ^{111}In has been proposed as a radiopharmaceutical for infection imaging (*8–11*). Studies in a similar rat model (*10*), as described in this report, showed ^{111}In-IgG to be better than both ^{67}Ga-citrate and ^{99m}Tc-HSA in delineating abscesses at 24 hr postinjection. As outlined in the present paper, similar results were described for ^{99m}Tc-liposomes when compared to these two conventional infection imaging agents. A major drawback of the use of labeled IgG in infection diagnosis is the use of ^{111}In. The abscess located in the thigh in the 3-hr ^{111}In-IgG image was not discernible from normal muscle due to high muscle background activity. Low muscle deposition is probably a factor leading to the high target-to-background ratios determined from the images for ^{99m}Tc-liposomes over images from ^{111}In-IgG and ^{67}Ga-citrate. This rat model would tend to indicate that ^{99m}Tc-liposomes may be more useful than ^{111}In-IgG during the early stages of infection diagnosis.

Although the image analysis was different, the overall target-to-background ratios were higher at 24 hr for ^{99m}Tc-liposomes than for ^{111}In-IgG. To get around the use of ^{111}In, chemical conjugation procedures to label polyclonal antibody and other proteins with ^{99m}Tc are being developed and tested as infection imaging agents (*12,13,42*). In a study directly comparing ^{99m}Tc-IgG with ^{111}In-IgG in the rat, ^{99m}Tc-IgG was found to wash out of the abscess, decreasing from 0.7% ID/g at 6 hr to 0.3% ID/g at 24 hr. On the contrary, ^{111}In-IgG held constant at 1.0% ID/g from 6 to 24 hr (*42*). In contrast to ^{99m}Tc-IgG results, the ^{99m}Tc-liposomes described in this article significantly increased in activity at the abscess from 0.2% ID/g at 6 hr to 0.5% ID/g at 24 hr. In addition, in the ^{99m}Tc-IgG study, approximately 58% of the ^{99m}Tc dose was cleared from the body by 24 hr compared to 14% of the dose with ^{99m}Tc-liposomes. A previous study with liposomes labeled with ^{99m}Tc-DTPA has also shown greater than 50% cumulative excretion of the ^{99m}Tc dose at 24 hr (*43*). It appears that the ^{99m}Tc-liposomes described in this article display biodistribution kinetics for infection imaging similar to that previously described for ^{111}In-IgG (*42*).

In a recent study by McAfee et al. (*41*), ^{111}In-leukocytes remained the best agent for infection imaging. One reason for this is the specific nature of the leukocyte at the area of infection when compared to other more nonspecific agents listed above, including the ^{99m}Tc-liposomes evaluated in this report. Yet, in certain situations the use of other agents over ^{111}In-leukocytes prevails. One such situation would be in the need for an easy screening procedure which could be used the same day as tracer administration. Labeling leukocytes with ^{99m}Tc-HMPAO (*14*) has been developed to alleviate the waiting period, but it does not alleviate the long and tedious labeling procedure. Also, the leakage of the ^{99m}Tc from leukocytes by 3 hr postinjection makes intra-abdominal abscess imaging difficult. Furthermore, withdrawing blood from AIDS patients or other individuals with low leukocyte counts remains an issue in the use of labeled leukocytes for infection imaging.

If further studies demonstrate that ^{99m}Tc-liposomes are effective for localizing infection in humans, they would have several inherent advantages over other agents used in the clinical setting today. The ability to package this agent to have on hand in emergency situations and the excellent image quality at 4 hr makes it a viable radiopharmaceutical. When compared with other infection imaging agents, ^{99m}Tc-liposomes have the advantage of being used as drug carriers. This ^{99m}Tc-liposome detection system could be important in determining the therapeutic success of antibiotics such as Gentamicin, Streptomycin and Amphotericin B encapsulated in liposomes (*44–47*). Although ^{99m}Tc-liposomes are nonspecific and would not replace ^{111}In-labeled leukocytes, ^{99m}Tc-liposomes could be a useful addition to the armamentarium of radiopharmaceuticals currently used for infection imaging (*48*) and warrants further investigation.

ACKNOWLEDGMENTS

The authors thank Cono Farias for his expertise in photographing the images for this paper. This project was funded by a grant from the Naval Medical Research and Development Command.

REFERENCES

1. Gerzof SG, Oates ME. Imaging techniques for infections in the surgical patient. *Surg Clin North Am* 1988;68:147–165.
2. Lavender JP, Lowe J, Bakere JR, et al. Gallium citrate scanning in neoplastic and inflammatory lesions. *Br J Radiol* 1971;44:361–366.
3. Thakur ML, Coleman RE, Welch MJ. Indium-111-labeled leukocytes for the localization of abscesses: preparation, analysis, tissue distribution and comparison with gallium-67 citrate in dogs. *J Lab Clin Med* 1977;89:217–228.
4. Rojas-Burke J. Health officials reacting to infection mishaps [Newsline]. *J Nucl Med* 1992;33:13N–14N.
5. Ginsberg M, Roberto R, Trujillo E, et al. HIV exposure during nuclear medicine procedures. *JAMA* 1992;268:1253–1254.
6. De Schrijver M, Streule K, Senekowitsch R, Fridrich R. Scintigraphy of inflammation with nanometer-sized colloidal tracers. *Nucl Med Commun* 1987;8:895–908.

7. Streule K, De Schrijver M, Fridrich R. ^{99m}Tc-labeled HSA-nanocolloid versus ^{111}In oxine-labelled granulocytes in detecting sketal septic process. *Nucl Med Commun* 1988;9:59–67.
8. Strauss HW, Fischman AJ, Khaw BA, et al. Detection of acute inflammation with immune imaging. In: Chatal JF, ed. *Monoclonal antibodies in immunoscintigraphy*. Boca Raton, FL: CRC Press; 1989:325–335.
9. Fischman AJ, Rubin RH, Khaw BA, et al. Detection of acute inflammation with ^{111}In-labeled nonspecific polyclonal IgG. *Semin Nucl Med* 1988;18: 335–344.
10. Rubin RH, Fischman AJ, Needleman M, et al. Radiolabeled, nonspecific, polyclonal human immunoglobulin in the detection of focal inflammation by scintigraphy: comparison with gallium-67-citrate and technetium-99m-labeled albumin. *J Nucl Med* 1989;30:385–389.
11. Rubin RH, Fischman AJ, Callahan RJ, et al. Indium-111-labeled nonspecific immunoglobulin scanning in the detection of focal infection. *N Engl J Med* 1989;321:935–940.
12. Abrams MJ, Juweid M, tenKate CI, et al. Technetium-99m-human polyclonal IgG radiolabeled via the hydrazino nicotinamide derivative for imaging focal sites of infection in rats. *J Nucl Med* 1990;31:2022–2028.
13. Thakur ML, DeFulvio J, Park CH, et al. Technetium-99m-labeled proteins for imaging inflammatory foci. *Nucl Med Biol* 1991;18:605–612.
14. Mountford PJ, Kettle AG, O'Doherty MJ, Coakley AJ. Comparison of technetium-99m-HMPAO leukocytes with indium-111-oxine leukocytes for localizing intraabdominal sepsis. *J Nucl Med* 1990;31:311–315.
15. Seltzer SE. The role of liposomes in diagnostic imaging. *Radiology* 1989; 171:19–21.
16. Caride VJ. Technical and biological considerations on the use of radiolabeled liposomes for diagnostic imaging. *Nucl Med Biol* 1990;17:35–39.
17. Lasic D. Liposomes. *American Scientist* 1992;80:20–31.
18. Phillips WT, Rudolph AS, Goins B, Timmons JH, Klipper R, Blumhardt R. A simple method for producing a technetium-99m-labeled liposome which is stable in vivo. *Nucl Med Biol* 1992;19:539–547.
19. Rudolph AS, Klipper RW, Goins B, Phillips WT. In vivo biodistribution of a radiolabeled blood substitute: ^{99m}Tc-labeled liposome encapsulated hemoglobin in an anesthetized rabbit. *Proc Natl Acad Sci USA* 1991;88: 10976–10980.
20. Ballinger JR, Reid RH, Gulenchyn KY. Technetium-99m HMPAO stereoisomers: differences in interaction with glutathione. *J Nucl Med* 1988;29: 1998–2000.
21. Neirinckx RD, Burke JF, Harrison RC, Forster AM, Andersen AR, Lassen NA. The retention mechanism of technetium-99m-HMPAO: intracellular reaction with glutathione. *J Cereb Blood Flow Metab* 1988;8:504–512.
22. Stewart JCM. Colorimetric determination of phospholipids with ammonium ferrothiocyanate. *Anal Biochem* 1980;104:10–14.
23. New RRC. Paper chromatography of labelled liposomes. In: New RRC, ed. *Liposomes: a practical approach*. New York, NY; IRL Press; 1990:265.
24. Petty C. *Research techniques in the rat*. Springfield, IL: Charles C. Thomas; 1982:66–70.
25. Frank DW. Physiological data of laboratory animals. In: Melby EC Jr, Altman NH, eds. *Handbook of laboratory animal science, volume III*. Boca Raton, FL: CRC Press, 1976:23–64.
26. Scherphof GL. In vivo behavior of liposomes: interactions with the mononuclear phagocyte system and implications for drug targeting. In: Juliano RL, ed. *Targeted drug delivery*. New York: Springer-Verlag; 1991:285–327.
27. McAfee JG. Editorial: what is the best method for imaging focal infections? *J Nucl Med* 1990;31:413–416.
28. Crowe JH, Crowe LM, Carpenter JF, et al. Interactions of sugars with membranes. *Biochim Biophys Acta* 1988;947:367–384.
29. Rudolph AS, Cliff RO. Dry storage of liposome-encapsulated hemoglobin: a blood substitute. *Cryobiology* 1990;27:585–590.
30. Rudolph AS. The freeze-dried preservation of liposome encapsulated hemoglobin: a potential blood substitute. *Cryobiology* 1988;25:277–284.
31. Morgan JR, Williams KE, Davies RL, Leach K, Thomson M, Williams LAP. Localisation of experimental staphylcoccal abscesses by ^{99m}Tc-technetium-labelled liposomes. *J Med Microbiol* 1981;14:213–217.
32. Morgan JR, Williams LA, Howard CB. Technetium-labelled liposome imaging for deep-seated infection. *Br J Radiol* 1985;58:35–39.
33. Barratt GM, Tuzel NS, Ryman BE. The labeling of liposomal membranes with radioactive technetium. In: Gregoriadis G, ed. *Liposome technology, volume II*. Boca Raton, FL: CRC Press; 1984:94–105.
34. Storm G, Oussoren C, Peeters PAM, Barenholz Y. Tolerability of liposomes in vivo. In: Gregoriadis G, ed. *Liposome technology, volume III*. Boca Raton, FL: CRC Press; 1993:345–383.
35. Lopez-Berestein G. Treatment of systemic fungal infections with liposomal-amphotericin B. In: Lopez-Berestein G, Fidler IJ, eds. *Liposomes in the therapy of infectious diseases and cancer*. New York: Alan R. Liss; 1988: 317–327.
36. Treat J, Greenspan AR, Rahman A. Liposome encapsulated doxorubicin preliminary results of phase I and phase II trials. In: Lopez-Berestein G, Fidler IJ, eds. *Liposomes in the therapy of infectious diseases and cancer*. New York, NY: Alan R. Liss; 1988:353–365.
37. Allen TM, Hansen C, Rutledge J. Liposomes with prolonged circulation times: factors affecting uptake by reticuloendothelial and other tissues. *Biochim Biophys Acta* 1989;981:27–35.
38. Woodle MC, Matthay KK, Newman MS, et al. Versatility in lipid compositions showing prolonged circulation with sterically stabilized liposomes. *Biochim Biophys Acta* 1992;1105:193–200.
39. Cliff RO, Ligler F, Goins B, Hoffmann P, Spielberg H, Rudolph AS. Liposome encapsulated hemoglobin: long term storage stability and in vivo characterization. *Biomat Art Cells Immob Biotech* 1992;20:619–626.
40. Beach MC, Morley J, Spiryda L, Weinstock SB. Effects of liposome encapsulated hemoglobin on the reticuloendothelial system. *Biomat Art Cells Immob Biotech* 1992;20:771–776.
41. McAfee JG, Gagne G, Subramanian G, Schneider RF. The localization of indium-111-leukocytes, gallium-67-polyclonal IgG and other radioactive agents in acute focal inflammatory lesions. *J Nucl Med* 1991;32:2126–2131.
42. Oyen WJG, Claessens RAMJ, van der Meer JWM, Corstens FHM. Biodistribution and kinetics of radiolabeled proteins in rats with focal infection. *J Nucl Med* 1992;33:388–394.
43. Espinola LG, Beaucaire J, Gottschalk A, Caride VJ. Radiolabeled liposomes as metabolic and scanning tracers in mice. II. In-111 oxine compared with Tc-99m DTPA, entrapped in multilamellar lipid vesicles. *J Nucl Med* 1979;20:434–440.
44. Swenson CE, Stewart KA, Hammett JL, Fitzsimmons WE, Ginsberg RS. Pharmacokinetics and in vivo activity of liposome-encapsulated gentamicin. *Antimicrob Agents Chemother* 1990;34:235–240.
45. Fierer J, Hatlen L, Lin JP, Estrella D, Mihalko P, Yau-Young A. Successful treatment using gentamicin liposomes of *Salmonella dublin* infections in mice. *Antimicrob Agents Chemother* 1990;34:343–348.
46. Mehta RT, Lopez-Berestein G. Effect of liposome encapsulation on toxicity and antifungal activity of polyene antibiotics. In: Lopez-Berestein G, Fidler IJ, eds. *Liposomes in the therapy of infectious diseases and cancer*. New York, NY: Alan R Liss; 1988:263–273.
47. Duzgunes N, Ashetar DR, Flasher DL, et al. Treatment of Mycobacterium avium-intracellulare complex infection in beige mice with free and liposome-encapsulated streptomycin: role of liposome type and duration of treatment. *J Infect Dis* 1991;164:143–151.
48. Corstens FHM, Claessens RAMJ. Imaging inflammation with human polyclonal immunoglobin: not looked for but discovered. *Eur J Nucl Med* 1992;19:155–158.